PAPER

Imaginary-time time-dependent density functional theory for periodic systems

IOP Publishing Journal of Physics: Condensed Matter
J. Phys.: Condens. Matter **33** (2021) 055903 (8pp) https://doi.org/10.1088/1361-648X/abbe7e

Imaginary-time time-dependent density functional theory for periodic systems

John McFarland[1] **and Efstratios Manousakis**[1,2]

[1] Department of Physics and National High Magnetic Field Laboratory, Florida State University, Tallahassee, FL 32306-4350, United States of America
[2] Department of Physics, National and Kapodistrian University of Athens, Panepistimioupolis, Zografos, 157 84 Athens, Greece

E-mail: swqecs@gmail.com and manousakis@gmail.com

Received 2 June 2020, revised 22 September 2020
Accepted for publication 5 October 2020
Published 5 November 2020

Abstract

Imaginary-time time-dependent density functional theory (it-TDDFT) has been proposed as an alternative method for obtaining the ground state within density functional theory (DFT) which avoids some of the difficulties with convergence encountered by the self-consistent-field (SCF) iterative method. It-TDDFT was previously applied to clusters of atoms where it was demonstrated to converge in select cases where SCF had difficulty with convergence. In the present work we implement it-TDDFT propagation for *periodic systems* by modifying the Quantum ESPRESSO (QE) package, which uses a plane-wave basis with multiple $\boldsymbol{k}$ points, and has the options of non-collinear and DFT + U calculations using ultra-soft or norm-conserving pseudo potentials. We demonstrate that our implementation of it-TDDFT propagation with multiple $\boldsymbol{k}$ points is correct for DFT + U non-collinear calculations and for DFT + U calculations with ultra-soft pseudo potentials. Our implementation of it-TDDFT propagation converges to the exact SCF energy (up to the decimal guaranteed by double precision) in all but one case where it converged to a slightly lower value than SCF, suggesting a useful alternative for systems where SCF has difficulty reaching the Kohn–Sham (KS) ground state. In addition, we demonstrate that more rapid convergence can be achieved if we use adaptive-size imaginary-time-steps for different kinetic-energy plane-waves.

Keywords: electronic structure, density functional theory, Quantum ESPRESSO, imaginary time evolution

(Some figures may appear in colour only in the online journal)

1. Introduction

Having excellent scalability, density functional theory (DFT) is widely used for electronic structure calculations in a variety of fields. Current implementations of DFT scale [1] as $O(N^2)$ with the number of electrons up to around 1000 electrons, and beyond that it scales as $O(N^3)$. It is based on the Hohenberg–Kohn theorem [2] of a one-to-one correspondence between the ground-state wavefunction and its charge density. Methods that search for the ground state seek the lowest energy solution where both the wavefunction and charge density are consistently calculated from each other.

The Kohn–Sham (KS) Hamiltonian is a single-particle Hamiltonian with a potential that is the sum of the Coulomb and the exchange–correlation potentials, with the former coming from the atomic cores and the electron charge-density [3]. The exchange–correlation potential is a universal functional of the charge density and, for the LDA implementation, is tuned to give the same energy-density dependence as that of an interacting-homogeneous electron-gas [4, 5].

The KS wave function is a set of single particle wave functions (KS states) that are occupied by one or two electrons for the non-collinear and collinear cases, respectively. When in the ground state, the KS states are the lowest-energy eigenvectors of the KS Hamiltonian. The KS ground state and Hamiltonian are required to be consistent with each other.

* Author to whom any correspondence should be addressed.

The KS ground state is typically reached by means of self-consistent-field (SCF) iterations [1]. With an initial charge density, a set of lowest eigenvectors of the KS Hamiltonian are first calculated, then occupation numbers (weights) are assigned to them, and afterwards a new charge density is calculated from the occupied eigenvectors. This density is usually mixed with densities from previous iterations to aid convergence [6].

It is well documented that SCF has difficulty converging for some systems. One cause is charge sloshing, where some orbitals continually fluctuate above and below the Fermi level causing their weights, and, thus, the charge density to also fluctuate. This is more prevalent for systems with many orbitals close to the Fermi level, such as metallic and large systems [7]. In addition, SCF will sometimes algorithmically converge (i.e., the charge density of subsequent iterations changes within a very small tolerance) to an excited state. While the usual solution is to start with different initial states, it is difficult to know if a converged state is the ground state or an excited one.

Common solutions to address convergence problems associated with fluctuations are mixing a smaller fraction of the calculated charge density with previous iterations and smearing the occupation numbers close to the Fermi level [8]. Other solutions include starting with different initial states and mixing a greater number of iterative charge densities. Although the ability to converge can be improved with such changes, it is difficult to know *a priori* what scheme to use, or even whether or not the algorithmically converged solution is the true KS ground state.

Recently, imaginary-time time-dependent density functional theory (it-TDDFT) propagation was proposed by Flamant *et al* [9] as a more reliable method for generating the KS ground state. They demonstrate its advantage for various cases of atomic clusters where the SCF iteration approach had difficulty converging to the KS ground-state. It-TDDFT is a modification of real-time time-dependent density functional theory (TDDFT), which is a long established approximation of dynamical quantum systems. [10] TDDFT improves calculations of excitation spectra [11] and has applications in quantum computing [12].

In the it-TDDF approach the KS orbitals are propagated in imaginary time with the KS Hamiltonian, while their orthonormalization is maintained. By extending a proof by Van Leeuwen [13] to it-TDDFT propagation, Flamant *et al* suggest that it-TDDFT propagation will eventually converge to the KS ground-state, provided that the initial state has a non-zero overlap with the KS ground-state, and that a sufficiently small time-step is used, which they adjust 'on-the-fly'. They demonstrate successful convergence to the ground states of Cu_{15} and Ru_{55} nanoclusters, where various SCF iteration schemes either converge to a higher energy state or fail to algorithmically converge at all. They used code based on SIESTA [14], which uses a localized basis.

In the present work we have applied it-TDDFT propagation to extensive (periodic) systems by modifying the open source package Quantum ESPRESSO (QE) [15, 16], which models periodic systems using a plane-wave basis. For periodic systems, KS orbitals take the Bloch form and essentially gain three additional dimensions corresponding to the values of the momentum $\boldsymbol{k}$ in the Brillouin zone. The charge density is calculated by integration of occupied band charge densities within the first Brillouin zone. We compare our results to SCF, where, since SCF has many implementation schemes, we try to use the default settings of QE as much as possible, and explicitly state what the settings are when they differ from the default values.

We first demonstrate that for simple systems our implementation gives the same ground-state energy and density as SCF up to 13 or more decimal places. Then we choose a metallic system (FCC copper) and demonstrate that we can reproduce the same ground-state energy, charge density, and Fermi surface as SCF. Then we examine the wall-time speeds of both it-ITDDFT and SCF and how they scale with system size. We also demonstrate that it-TDDFT can find a state with lower energy than SCF.

Our implementation can be found at https://github.com/Walkerqmc/ITDDFT_for_QE and, therefore, is now part of the public domain to be applied in cases where SCF loops appear to have difficulty reaching a fully converged ground state or when it is desirable to validate by a very different method that SCF iterations have reached the true DFT ground state. In addition to our work, the reader may find the popular open-source software package QuTiP useful, which studies the time-dependent properties of quantum open systems [17].

The paper is organized as follows. In section 2 we discuss our formulation of the problem and how it has been implemented using the QE. In section 3 we apply the method on selected systems and demonstrate that our implementation of it-TDDFT propagation for periodic systems reproduces SCF results for the ground-state energy, density, and Fermi surface, except in one case where it finds a lower energy state. In section 4 we present our main conclusions.

2. Imaginary time propagation and implementation for Quantum ESPRESSO

The ground-state wavefunction within DFT consists of single-particle orbitals $|\psi_m\rangle$. From these we can define a set of orthonormalized states, $|\phi_i\rangle$, spanning the same space as occupied orbitals, through a well-defined orthonormalization procedure (such as Gramm–Schmidt). With these we define the charge density ρ by

$$\rho(\mathbf{r}) = \sum_m \langle\phi_m|\boldsymbol{r}\rangle\langle\boldsymbol{r}|\phi_m\rangle = \mathrm{Tr}_{\mathrm{occ}}\{|\mathbf{r}\rangle\langle\mathbf{r}|\}, \tag{1}$$

where the trace is over the subspace spanned by the occupied orbitals. Thus the density is a function of only the subspace spanned by the single-particle orbitals $|\psi_m\rangle$, and not the particular choice of the basis set.

The KS Hamiltonian is a function of ρ and can be used to propagate each orbital in imaginary time $\tau = it$ according to the differential equation [9]

$$\frac{\mathrm{d}|\psi_m\rangle}{\mathrm{d}\tau} = -\mathrm{H}[\rho]\,|\psi_m\rangle\,, \tag{2}$$

where $\rho(\tau)$ is the instantaneous density defined by equation (1). By integrating both sides of this equation for a very small time-step $\Delta\tau$, we obtain the forward Euler propagator used in our work

$$|\psi_m(\tau+\Delta\tau)\rangle = (\mathrm{I} - \Delta\tau \mathrm{H}[\rho(\tau)])\,|\psi_m(\tau)\rangle\,. \tag{3}$$

Orthonormalization of $|\psi_m\rangle$ is not preserved with it-ITDDFT propagation. However, if we orthonormalize at any time during propagation, it will not change the final space spanned by $|\psi_m\rangle$ and thus the final ρ defined by equation (1). We are thus free to orthonormalize $|\psi_m\rangle$ every iteration, so that we may calculate ρ directly from $|\psi_m\rangle$ every time we update the Hamiltonian. We have used the Gram–Schmidt method, which successively orthonormalizes a set of orbitals, where if orbitals with index less than m are orthonormal, the orbital $|\psi_m(t)\rangle$ is orthonormalized by the transformations

$$|\psi_m\rangle \Rightarrow |\psi_m\rangle - \sum_{n<m} |\psi_n\rangle\,\langle\psi_n|\psi_m\rangle, \tag{4}$$

$$|\psi_m\rangle \Rightarrow \frac{|\psi_m\rangle}{\sqrt{\langle\psi_n|\psi_m\rangle}}. \tag{5}$$

Quantum ESPRESSO (QE) is used to solve the KS equations for periodic systems. The KS orbitals are the Bloch states $\psi_{n\boldsymbol{k}}(\boldsymbol{r}) = \mathrm{e}^{-\mathrm{i}\boldsymbol{k}\cdot\boldsymbol{r}} u_{n\boldsymbol{k}}(\boldsymbol{r})$, where u is periodic and expanded in a plane-wave basis. The index $\mathbf{k}$ forms grid points within the first Brillouin zone. Bloch states at different $\boldsymbol{k}$ are characterized by different kinetic energy of the plane-waves, allowing an effective $\boldsymbol{k}$-dependent Hamiltonian which QE uses to solve the eigenvalue equation

$$\mathrm{H}\,|\psi_{n\boldsymbol{k}}\rangle = \epsilon_{n\boldsymbol{k}}\,|\psi_{n\boldsymbol{k}}\rangle \tag{6}$$

separately for each value of $\boldsymbol{k}$ during SCF iterations.

The next step of the iteration is to calculate the charge density and total energy, and to do this occupation numbers called weights $w_{n\boldsymbol{k}}$ are assigned to the Block wave functions. The weights are normalized so they yield the correct total charge of the valence electrons. Generally, the bands up to Fermi level are occupied, with possible smearing near the transition from occupied to unoccupied states for metals. Smearing is done to smooth the effect of a finite number of $\boldsymbol{k}$ points and to prevent fluctuations.

The charge density and band energy are then calculated as follows

$$\rho(\mathbf{r}) = \sum_{n\boldsymbol{k}} w_{n\boldsymbol{k}} \langle\psi_{n\boldsymbol{k}}|\boldsymbol{r}\rangle\langle\boldsymbol{r}|\psi_{n\boldsymbol{k}}\rangle, \tag{7}$$

$$E_{\mathrm{band}} = \langle\Psi|\mathrm{H}|\Psi\rangle = \sum_{n\boldsymbol{k}} w_{n\boldsymbol{k}}\epsilon_{n\boldsymbol{k}}. \tag{8}$$

Most $\boldsymbol{k}$ points can be grouped into sets related by symmetry transformations that preserve charge density and energy. For efficiency, QE reduces the $\boldsymbol{k}$ points in such a set to a single one with a larger weight. After the charge density is calculated, it is typically mixed with a linear combination of charge densities from previous iterations to aid convergence.

We have implemented it-TDDFT by modifying the SCF iterations in the QE package. Instead of solving equation (6), we apply the forward Euler propagator given by equation (3) to each of the Bloch states. Gram–Schmidt orthonormalization is then performed separately for each group of Bloch states that have the same $\boldsymbol{k}$ index, since states with different $\boldsymbol{k}$ remain orthogonal over all cells after propagation. We calculate the band energy as

$$\epsilon_{n\boldsymbol{k}} = \langle\psi_{n\boldsymbol{k}}|\,\mathrm{H}\,|\psi_{n\boldsymbol{k}}\rangle\,. \tag{9}$$

The weights of equation (8) must then be assigned to the Bloch states, and the method to do so must allow the transition of electrons to different $\boldsymbol{k}$-points if the ground state has a different $\boldsymbol{k}$-point distribution from the initial state. We experimented with two weight-assigning methods. One was to simply let one of the QE subroutines assign weights based on the $\epsilon_{n\boldsymbol{k}}$ values. This, however, does not yield proper imaginary-time dynamics, since electrons can immediately transition from one Bloch state to another if the states move above and below the Fermi level during the it-TDDFT propagation, which can result in charge sloshing.

We wanted accurate imaginary-time dynamics to avoid charge sloshing and the use of smearing, and because it may be possible to calculate the density of excited states from the evolution of energy. We therefore produced another method that assigns weights in a way that approximates imaginary-time dynamics. Since it-TDDFT propagation does not change the $\boldsymbol{k}$ value of a Bloch state, this method drops the requirement that a KS state is a Bloch state, and instead uses Bloch states as a basis to superimposes the KS states over. In this case propagation with equation (3) will move the charge of a KS state from higher energy Bloch states to lower energy ones. Thus by initially superimposing the KS states among all possible $\boldsymbol{k}$-points, we allow it-TDDFT propagation to shift the electron $\boldsymbol{k}$-point distribution in a way that lowers energy.

We implement this by introducing a new set of coefficients $c_{in\boldsymbol{k}}$ that relate the Bloch states in QE $|\psi_{n\boldsymbol{k}}\rangle$ to the KS states $|\phi_i\rangle$,

$$|\phi_i\rangle = \sum_{n\boldsymbol{k}} c_{in\boldsymbol{k}} |\psi_{n\boldsymbol{k}}\rangle. \tag{10}$$

We initialize the $c_{in\boldsymbol{k}}$ values by first selecting them at random, then we Grahm–Schmidt orthonormalize them so that $\langle\phi_i|\phi_j\rangle = \delta_{ij}$. The KS states are then it-TDDFT propagated as

$$|\phi_i(\tau+\Delta\tau)\rangle = \sum_{n\boldsymbol{k}} c_{in\boldsymbol{k}}\,(\mathrm{I} - \Delta\tau\mathrm{H}[\rho(\tau)])\,|\psi_{n\boldsymbol{k}}(\tau)\rangle\,, \tag{11}$$

and then orthonormalized.

To orthonormalize, we first give the KS states an orthonormal basis by orthonormalizing the $|\psi_{n\boldsymbol{k}}\rangle$ states while simultaneously keeping the $|\phi_i\rangle$ states fixed by adjusting the $c_{in\boldsymbol{k}}$ coefficients. This is done by building a $\boldsymbol{k}$-point dependent matrix during orthonormalization which later operates on the $c_{in\boldsymbol{k}}$ coefficients. After this we Gram–Schmidt orthonormalize the $c_{in\boldsymbol{k}}$ coefficients, and thus the KS states.

To calculate the charge density, we have employed an approximation that becomes exact as the wavefunction approaches the exact KS ground state. Combining index n and $\boldsymbol{k}$ to an index m, we calculate the weights as

$$w_m = \sum_i |c_{im}|^2, \tag{12}$$

and use equations (7) and (8) to calculate charge density and band energy. The correct charge density is given by

$$\rho(\boldsymbol{r}) = \sum_i \langle \phi_i | \boldsymbol{r} \rangle \langle \boldsymbol{r} | \phi_i \rangle, \tag{13}$$

which by mere substitution becomes

$$\rho(\boldsymbol{r}) = \sum_i \sum_{m'} \sum_m c^*_{im'} c_{im} \langle \psi_{m'} | \boldsymbol{r} \rangle \langle \boldsymbol{r} | \psi_m \rangle. \tag{14}$$

When approaching the KS ground state, the number of both our KS states and occupied Block states become equal. This makes c_{im} a unitary matrix resulting in $\sum_i c^*_{im'} c_{im} = \delta_{m,m'}$, converging to our approximation for the charge density

$$\rho(\boldsymbol{r}) = \sum_i \sum_m |c_{im}|^2 \langle \psi_m | \boldsymbol{r} \rangle \langle \boldsymbol{r} | \psi_m \rangle. \tag{15}$$

As explained, QE reduces the bands of a set of $\boldsymbol{k}$ points related by symmetry to one $\boldsymbol{k}$ point with accumulated weight $w_{\boldsymbol{k}}$, where $w_{\boldsymbol{k}}$ is the weight of a fully occupied Bloch state. To account for this extra weight we assign additional $c_{in\boldsymbol{k}}$ coefficients to the bands of a reduced $\boldsymbol{k}$ point, equal to the $w_{\boldsymbol{k}}$ of that point divided by the greatest common factor of all $w_{\boldsymbol{k}}$ values. We also reduced the number of $c_{in\boldsymbol{k}}$ coefficients by freezing the electrons well below the Fermi surface.

We implemented it-TDDFT for both norm-conserving [18] and ultra-soft [19] pseudo-potentials (USPPs). The formalism presented so far was for the former. USPPs let us use less plane-waves (i.e., a lower energy cut-off) by smoothing out the wavefunction within cutoff radii of the nuclei. The price that we pay for doing this is that the Bloch states are not orthonormal, but instead obey the condition

$$\langle \psi_{n\boldsymbol{k}} | \mathrm{S} | \psi_{n'\boldsymbol{k}'} \rangle = \delta_{n\boldsymbol{k},n'\boldsymbol{k}'}. \tag{16}$$

S can be thought of as mapping the bands $|\psi_{n\boldsymbol{k}}\rangle$ to a set of orthonormal bands $|\tilde{\psi}_{n\boldsymbol{k}}\rangle$, with $|\tilde{\psi}_{n\boldsymbol{k}}\rangle = \mathrm{S}^{\frac{1}{2}} |\psi_{n\boldsymbol{k}}\rangle$.

We can obtain the equations for the bands of USPPs from the above equations for orthonormal bands with the substitutions $|\psi_{n\boldsymbol{k}}\rangle \to \mathrm{S}^{\frac{1}{2}} |\psi_{n\boldsymbol{k}}\rangle$ and $\mathrm{H} \to \mathrm{S}^{-\frac{1}{2}} \mathrm{H} \mathrm{S}^{-\frac{1}{2}}$, provided S is constant. As an example, with substitutions and multiplying the left-hand-side of equation (3) by $\mathrm{S}^{-\frac{1}{2}}$, the forward Euler propagator becomes

$$|\psi_m(\tau + \Delta\tau)\rangle = \left(\mathrm{I} - \Delta\tau \mathrm{S}^{-1} \mathrm{H}[\rho(\tau)]\right) |\psi_m(\tau)\rangle \,. \tag{17}$$

We implement equation (17) by operating on the bands first with a Hamiltonian subroutine and then an inverse S subroutine found in the QE package. The latter does not support non-collinear calculations, which is where plane-waves and spin are combined to a single basis to enable relativistic spin orbit coupling [20]. Thus, we have only implemented it-TDDFT with USPPs for the collinear case.

Our implementation of it-TDDFT naturally works for DFT + U calculations, which model the effect of correlations by introducing an extra energy term U when two electrons occupy the same atomic site [21]. In this case the Hamiltonian depends also on occupation numbers n_j, calculated by

$$n_j = \sum_{n\boldsymbol{k}} \langle \psi_{n\boldsymbol{k}} | \chi_j \rangle \langle \chi_j | \psi_{n\boldsymbol{k}} \rangle, \tag{18}$$

where $|\chi_j\rangle$ are local orbitals of atoms that a Hubbard U was applied to.

The size of the time-step is an important parameter in the it-TDDFT propagation. Generally one wants the largest value that still results in monotonically decreasing energy. Flamant *et al* [9] adjusted the time-step on the fly by decreasing it when the total energy increased and increasing it otherwise. Our experience with this variable time-step was that in some cases it would constantly decrease to effectively zero, never resulting in monotonically decreasing energy. We instead set the time-step equal to one divided by the maximum plane-wave kinetic energy. Since if the time-step is larger than twice this, the propagator of equation (3) will multiply the highest kinetic-energy plane-waves with a value less than negative one, resulting in exponential increase. Propagators that can use a larger time step are a possible extension of this project.

We have also developed a method that uses a larger time-step for lower energy plane-waves. This propagation alone would result in disproportionately larger expansion of the lower-energy plane-waves, so we counter it by dividing each plane wave by the expected change in its magnitude given the associated time step and band energy. Specifically, we use the propagator

$$|\psi_i\rangle \Rightarrow \sum_g |g\rangle\langle g| \frac{\mathrm{I} - \Delta\tau_g \mathrm{H}}{1 - \Delta\tau_g \epsilon_i} |\psi_i\rangle \,, \tag{19}$$

where the states $|g\rangle$ stand for the plane-wave, and where

$$\epsilon_i = \langle \psi_i | \mathrm{H} | \psi_i \rangle. \tag{20}$$

Namely, as the bands approach eigenvectors of H, the propagator of equation (19) approaches normalized imaginary-time propagation. We set the plane-wave dependent time-step to the inverse of the plane-wave kinetic energy with a maximum cut-off. Orthonormalization and the calculation of weights are performed in the same way as already discussed.

3. Results

3.1. Benchmarking our implementation

We present the results of the application of our implementation of it-TDDFT within QE on various systems, demonstrating that it can converge to the same energy as SCF within the desired level of accuracy. In addition we measured the difference between charge densities of it-TDDFT and SCF produced ground states for the systems studied using the metric

$$D[n, n_0] = \frac{1}{2} \int |n(\boldsymbol{r}) - n_0(\boldsymbol{r})| \mathrm{d}^3\boldsymbol{r}, \tag{21}$$

where $\int n(\boldsymbol{r}) \mathrm{d}^3\boldsymbol{r}$ equals the number of electrons.

Table 1. Charge-density difference as defined by equation (21) (second column) and ground state energy obtained with SCF (third column) and it-TDDFT (fourth column) for three systems. The ground state energy is in agreement to 13 or more decimal places. Calculations were collinear with ultra-soft pseudo-potentials.

System	$D[n, n_0]$	SCF energy (Ry)	it-TDDFT energy (Ry)
Silicon	1.52×10^{-15}	−15.853 571 686 0612	−15.853 571 686 0612
Diamond	1.09×10^{-14}	−22.771 396 652 4047	−22.771 396 652 4047
Graphene	1.49×10^{-13}	−22.791 839 022 835	−22.791 839 022 83

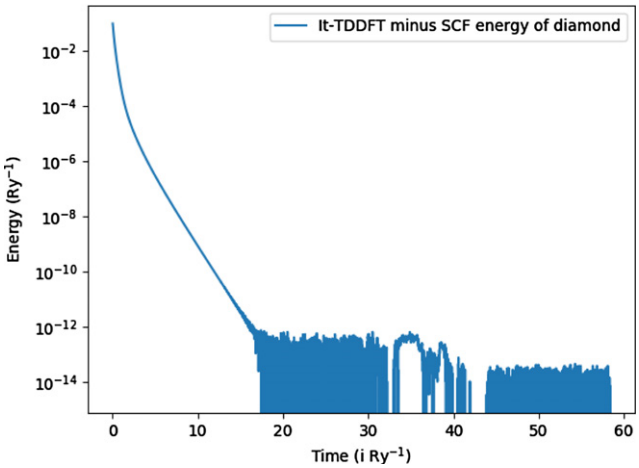

Figure 1. Energy of it-TDDFT propagated diamond minus SCF energy.

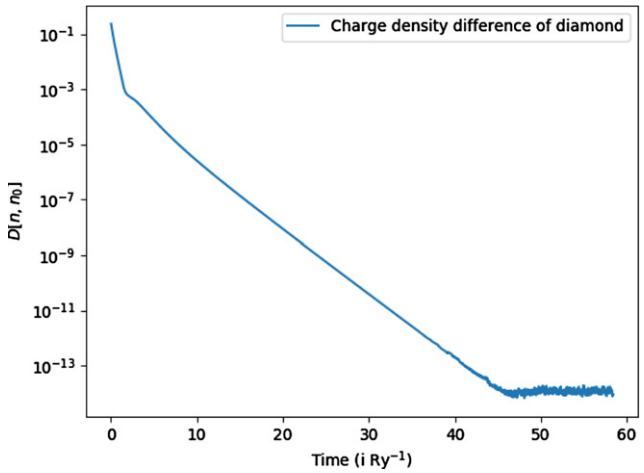

Figure 2. Charge-density difference between it-TDDFT propagated diamond and the SCF ground state, as defined by equation (21).

In table 1 we compare the results of the application of it-TDDFT on Si, diamond, and graphene to those obtained using SCF iterations. Notice that the energy and the charge density $n(\mathbf{r})$ in both calculations agree to at least 13 decimal places. This is a strong indication that our implementation of it-TDDFT within QE is correct. We plot the energy and charge density difference as a function of imaginary-time in figures 1 and 2 respectively. Notice that the energy and density converge exponentially and quickly to their SCF values up to 13-decimal points of accuracy and that their difference from the SCF values falls within the numerical noise.

Next we examine how the wall-time of a single-threaded iteration of it-TDDFT changes with system volume and plane-wave cut-off energy, and compare our results to SCF. We tested different super cells of platinum and silicon, with electron numbers ranging from 32 to 576, and with plane-wave cut-off energies of 20, 40, and 60 Rydbergs. We present the average time per iteration in table 2. It-TDDFT iteration time roughly scaled as $O(N^3)$ with electron number for most of our tested range, though the scaling was less at the lower edge of electron number. SCF had similar scaling, and we did not notice any trends in the ratio of SCF iteration time to it-TDDFT iteration time as we varied system volume or plan-wave cut-off energy.

SCF iteration time for all runs was on averaged 2.9 times greater than it-TDDFT, however SCF still converged to the ground state significantly faster than it-TDDFT for silicon and platinum when sufficient smearing was used to prevent fluctuations. The stability criterion of the forward Euler propagator used by it-TDDFT prevents the time step from exceeding roughly twice the inverse of the plane-wave cut-off energy, resulting in slow convergence speed relative to SCF which decreases with increasing cut-off. Other propagators, such as first-order Crank–Nicolson [22] or implicit Euler, may allow a larger time step and are a possible future improvement.

In table 3 we compare the wall-times required by it-TDDFT and SCF to lower the energy to within different tolerances for different sized systems. We present the ratio R of it-TDDFT to SCF wall-times to reach the displayed tolerance Δ. We define Δ as the magnitude of the difference between the energy reached and the ground state energy, divided by the ground state energy. As can be seen the wall-time of It-ITDDFT is considerably greater than SCF, and the ratio R increases as the energy gets closer to the ground state. R also decreases with increasing cell size (electron number). It should be noted that SCF energy does not decrease with every iteration, though it does for the good majority. Columns in the table correspond to different numbers of SCF iterations. While speed is not the advantage of it-TDDFT over SCF, there are advantages discussed in the following subsection.

3.2. *It-TDDFT can be advantageous to SCF*

In figure 3 we show it-TDDFT propagation can converge to a lower energy for the non-collinear case of a single atom

Table 2. Comparison of the wall-time of an iteration of SCF (fourth column) and it-TDDFT (fifth column) for different sized super cells of platinum and silicon, with various plan-wave kinetic-energy cut-offs (third column). Wall-times were single threaded and averaged over a run. Calculations were single *k*-point, collinear, with norm-conserving pseudo-potentials and no Hubbard U.

Element	Electron number	Cut-off (Ry)	SCF time (sec)	It-TDDFT time (sec)	Ratio
Pt	72	20.0	0.1465	0.036 58	4
Pt	72	40.0	0.2251	0.091 89	2.45
Pt	72	60.0	1.872	0.2337	8.01
Pt	144	20.0	3.654	0.2765	13.2
Pt	144	40.0	7.705	1.57	4.91
Pt	144	60.0	9.229	2.14	4.31
Pt	288	20.0	16.43	3.827	4.29
Pt	288	40.0	25.22	5.349	4.71
Pt	288	60.0	28.45	10.02	2.84
Pt	576	20.0	152.5	14.53	10.5
Pt	576	40.0	89.36	36.13	2.47
Pt	576	60.0	209.4	59.05	3.55
Si	32	20.0	0.047 66	0.029 12	1.64
Si	32	40.0	0.3676	0.141	2.61
Si	32	60.0	0.4181	0.1982	2.11
Si	64	20.0	0.4509	0.214	2.11
Si	64	40.0	2.085	1.796	1.16
Si	64	60.0	5.623	3.12	1.8
Si	128	20.0	1.909	0.6539	2.92
Si	128	40.0	8.693	1.815	4.79
Si	128	60.0	18.07	3.358	5.38
Si	256	20.0	27.07	7.679	3.53
Si	256	40.0	77.2	21.53	3.59
Si	256	60.0	195.1	39.1	4.99

Table 3. The ratio R of it-TDDFT to SCF wall-times required to reach various energy tolerances Δ. See text for definitions of R and Δ. Calculations are done for different cell sizes of collinear silicon with four *k*-points, 40(Ry) plane-wave cut-off, norm-conserving pseudo-potentials, and no Hubbard U. Columns correspond to 2, 4, and 7 SCF iterations.

Electron number	R	Δ	R	Δ	R	Δ
8	16.3	1.6×10^{-4}	38.3	1.7×10^{-7}	48.5	4.3×10^{-10}
32	10.4	1.4×10^{-4}	14.6	4.7×10^{-6}	36.6	6.1×10^{-9}
64	9.5	1.4×10^{-4}	13.7	4.6×10^{-6}	32.8	3.0×10^{-9}
128	10.0	1.4×10^{-4}	13.0	4.5×10^{-6}	29.7	1.1×10^{-9}

cell of FCC copper with 63 *k*-points and a Hubbard U of 2 eV. The it-TDDFT energy was −365.089 15(Ry), as compared to −365.089 14(Ry) produced by SCF. The difference in it-TDDFT and SCF charge densities as defined by equation (21) was 8.67×10^{-6}(Ry). SCF and it-TDDFT calculations used the default settings of QE with norm-conserving pseudo-potentials, a 0.01 value of the Gaussian spreading (smearing), a 0.3 mixing factor for SCF, and a constant time step for it-TDDFT.

Other cases where it-TDDFT converges to a lower energy than SCF, indicating that the latter has difficulty converging to the correct KS ground state, were presented in reference [9]. Such cases are a reason one might find our application of the it-TDDFT method useful, namely, when SCF has difficulty to converge. Our application may also be useful if one wishes use little or no of smearing. The smearing width is generally set as small as needed since it introduces an un-physical effect. However, it is difficult to estimate the optimal value, which may require convergence testing.

3.3. Additions to the method

Next, in figure 4 we compare two methods of implementing it-TDDFT. One using superposition of Bloch states, i.e., using equation (10), to calculate occupations, the other using the standard QE method. The system used for comparison is collinear GaAs with a Hubbard U of 2 eV using ultra-soft pseudo potentials. Notice in figure 4 that the superimposed Bloch states converge to exactly the same energy as SCF. The speed of convergence of the superposition method is slower.

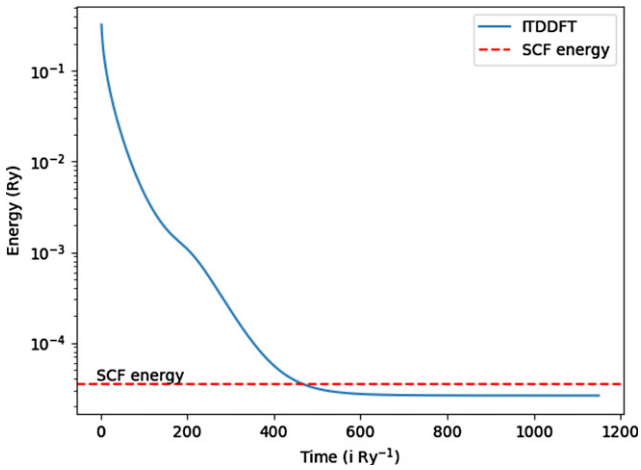

Figure 3. Relative energies of FCC copper it-TDDFT propagated with a $2.73 \times 10^{-2}\,\mathrm{Ry}^{-1}$ time-step. Occupations are calculated with a QE method. This calculation uses norm-conserving pseudo-potentials, 63 reduced k-points, and a 2 eV rotationally invariant Hubbard U implementation of Liechtenstein *et al* [23].

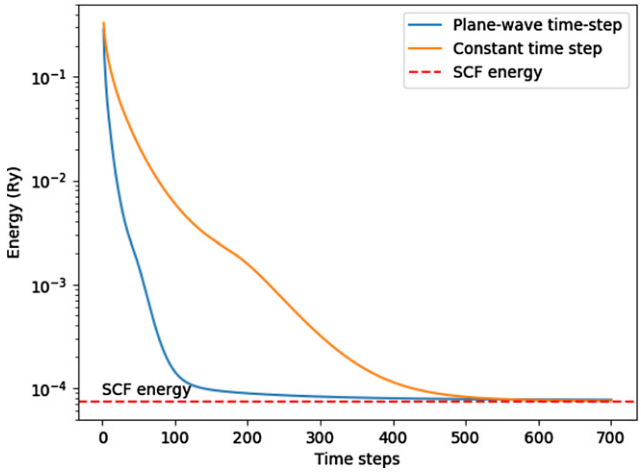

Figure 5. Relative energy of it-TDDFT propagated FCC copper. Orange has a constant time-step equal to 1.9 divided by the maximum plane-wave kinetic energy, or $2.73 \times 10^{-2}\,\mathrm{Ry}^{-1}$. Blue has a plane-wave dependent time-step equal to 1 divided by the plane-wave kinetic energy with a maximum cut off. The calculation is collinear with no Hubbard U.

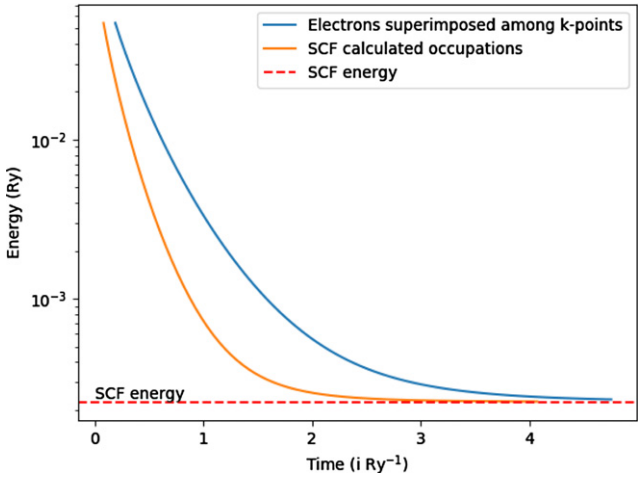

Figure 4. Relative energy of GaAs it-TDDFT propagated with a $2.73 \times 10^{-2}\,\mathrm{Ry}^{-1}$ time-step. For blue, electrons are superimposed among k-points. For orange, occupations are calculated with a QE method. Calculation uses a Hubbard U of 2 eV, ultra-soft-pseudo potentials, and 8 reduced k-points.

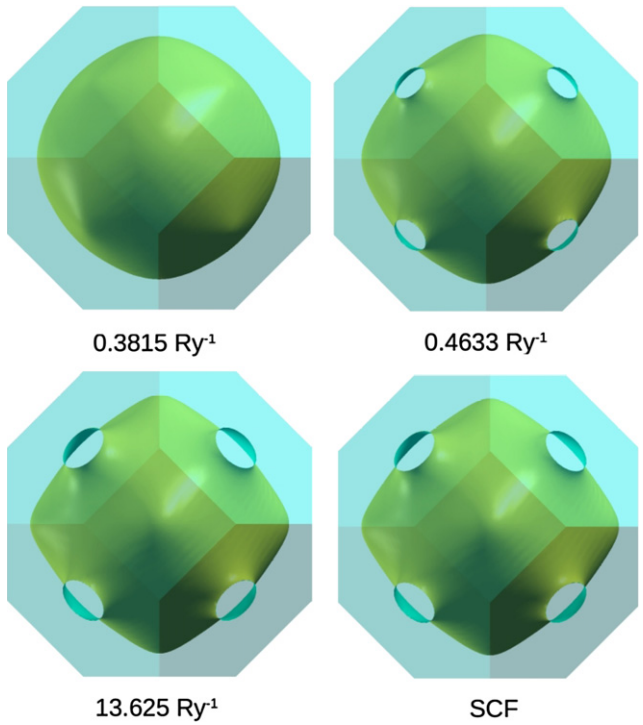

Figure 6. Imaginary time evolution of the Fermi surface of copper compared to that of SCF.

This can be explained by the small energy difference between different k-point distributions of the electrons, resulting in a slow shift of charge between k-points (whereas QE calculated occupations can instantly shift charge).

While the superposition method is slower, it does not require smearing and could be useful when trying to converge to the correct Fermi surface if occupations near the Fermi energy shift from iteration to iteration due to small energy differences, i.e., charge sloshing. Also, for the copper system of figure 3, the superposition method converged to an energy of −365.089 21(Ry), less than both SCF and it-TDDFT with the standard QE method for calculating weights, which were −365.089 14(Ry) and −365.089 15(Ry) respectively.

Next, in figure 5 we compare the speeds of the plane-wave dependent time-step with a constant time step for FCC copper. Both converge close to the SCF ground state, with the plane-wave dependent time-step converging faster. However, for some systems the plane-wave dependent time step fails to converge. Finally, in figure 6 we show that the Fermi surface of copper evolves to the same Fermi surface produced by SCF.

4. Conclusions and discussion

Imaginary time propagation is an alternative method for calculating the DFT ground state, and may be useful for large metallic systems or any others where the standard SCF has difficulty converging to the correct ground state [9]. We have implemented it for periodic systems by modifying the open source package Quantum ESPRESSO. Our implementation uses a plane-wave basis with the options of multiple $\boldsymbol{k}$-points, DFT + U, collinear or non-collinear, and norm-conserving or ultra-soft pseudo-potentials. As we demonstrate, our implementation reproduces within the computer accuracy the results for the ground-state energy and density distribution obtained by SCF. We also demonstrate that the present method can approach closer to the KS ground-state than the SCF in certain systems. Therefore, it is an alternative to the SCF iterative scheme to be at the disposal of the researcher who is interested in properties of periodic systems.

We presented three variations of this implementation: (a) one that calculates the occupation numbers of the KS states using a QE subroutine, (b) one that calculates the occupation numbers by modeling the evolution of KS states that are superimposed over $\boldsymbol{k}$ points, and (c) another implementation that propagates lower kinetic energy plane-waves with a larger time-step. We demonstrate the advantages and disadvantages of these three implementations by applying them to several systems.

The source code of our implementation can be found at https://github.com/Walkerqmc/ITDDFT_for_QE and, therefore, it can be easily applied in cases where the standard methodology of SCF cannot reach a fully converged ground state or for other reasons, such as, when it is desirable to make sure that SCF iterations have reached the true DFT ground state.

Acknowledgments

We wish to thank Dr Grigory Kolesov and Cedric Flamant for useful discusions. This work was supported in part by the US National High Magnetic Field Laboratory, which is funded by NSF DMR-1157490 and the State of Florida.

ORCID iDs

Efstratios Manousakis https://orcid.org/0000-0002-6052-7790

References

[1] Kresse G and Furthmüller J 1996 *Phys. Rev.* B **54** 11169
[2] Hohenberg P and Kohn W 1964 *Phys. Rev.* **136** B864
[3] Kohn W and Sham L J 1965 *Phys. Rev.* **140** A1133
[4] Ceperley D M and Alder B J 1980 *Phys. Rev. Lett.* **45** 566
[5] Štich I, Car R, Parrinello M and Baroni S 1989 *Phys. Rev.* B **39** 4997
[6] Pulay P 1980 *Chem. Phys. Lett.* **73** 393
[7] Anglade P-M and Gonze X 2008 *Phys. Rev.* B **78** 045126
[8] Rabuck A D and Scuseria G E 1999 *J. Chem. Phys.* **110** 695
[9] Flamant C, Kolesov G, Manousakis E and Kaxiras E 2019 *J. Chem. Theor. Comput.* **15** 6036–45
[10] Peuckert V 1978 *J. Phys. C: Solid State Phys.* **11** 4945
[11] Bauernschmitt R and Ahlrichs R 1996 *Chem. Phys. Lett.* **256** 454
[12] Gaitan F and Nori F 2009 *Phys. Rev.* B **79** 205117
[13] Van Leeuwen R 2001 *Int. J. Mod. Phys.* B **15** 1969
[14] Soler J M, Artacho E, Gale J D, García A, Junquera J, Ordejón P and Sánchez-Portal D 2002 *J. Phys.: Condens. Matter* **14** 2745
[15] Giannozzi P *et al* 2009 *J. Phys.: Condens. Matter* **21** 395502
[16] Giannozzi P *et al* 2017 *J. Phys.: Condens. Matter* **29** 465901
[17] Johansson J R, Nation P D and Nori F 2012 *Comput. Phys. Commun.* **183** 1760–72
[18] Hamann D R, Schlüter M and Chiang C 1979 *Phys. Rev. Lett.* **43** 1494
[19] Vanderbilt D 1990 *Phys. Rev.* B **41** 7892
[20] Kubler J, Hock K-H, Sticht J and Williams A R 1988 *J. Phys. F: Met. Phys.* **18** 469
[21] Anisimov V I, Zaanen J and Andersen O K 1991 *Phys. Rev.* B **44** 943
[22] Qian X, Li J, Lin X and Yip S 2006 *Phys. Rev.* B **73** 035408
[23] Shick A B, Liechtenstein A I and Pickett W E 1999 *Phys. Rev.* B **60** 10763